Variational Effective Index Method for 3D Vectorial Scattering Problems in Photonics: TE Polarization

O. V. Ivanova[1], **R. Stoffer**[2], **L. Kauppinen**[1], **and M. Hammer**[1]

[1]MESA+ Institute for Nanotechnology, University of Twente, Enschede, The Netherlands
[2]Phoenix Software, Enschede, The Netherlands

Abstract— In order to reduce the computational effort we develop a method for 3D-to-2D dimensionality reduction of scattering problems in photonics. Contrary to the 'standard' Effective Index Method the effective parameters of the reduced problem are always rigorously defined using the variational technique, based on the vectorial 3D Maxwell equations. Results for a photonic crystal slab waveguide show that this approach predicts the location of the bandgap and other spectral features much more precisely than any 'standard' EIM approximation.

1. INTRODUCTION

Fully vectorial 3D simulations of photonic components are often almost prohibitively CPU-time and memory intensive, so one would opt for reduced models that capture the essence of the full 3D structure, while being computationally much more efficient. Traditionally, integrated optics designers use a technique called the Effective Index Method (EIM) [1, 4, 7] to reduce simulations of 3D structures to two spatial dimensions. However, frequently, as is the case for photonic crystal slabs (Figure 1, left), the effective parameters for the 2D simulation are only rather ambiguously defined, i.e., rely more or less on guesswork. Here we have developed a mathematical formulation that allows to a priori derive these parameters when going from 3D to 2D based on a sound variational reasoning (Variational EIM, VEIM). This is achieved by approximating the total 3D vectorial electromagnetic field along one spatial dimension by a suitable 1D mode profile. Then, by means of a variational procedure, the field distribution in the other two dimensions is found, such that the product of these two fields represents as good as possible the true 3D vectorial solution. On the boundaries of the computational domain in 2D we use combined Transparent Influx Boundary Conditions with Perfectly Matched Layers in order to allow influx into the domain to be prescribed and radiation to freely pass through the computational window boundaries. Results for a photonic crystal slab waveguide show that this approach predicts the location of the bandgap and other spectral features much more precisely than any guesses using a 'standard' EIM.

2. FORMULATION OF SCATTERING PROBLEMS IN OPTICS

The time-harmonic propagation of a given optical influx with frequency ω through a medium, characterized by the refractive index distribution $n(x, y, z)$, is governed by the Maxwell curl equations

$$\nabla \times \mathbf{E} = -\mathrm{i}\,\omega\mu_0\mu\mathbf{H}, \quad \nabla \times \mathbf{H} = \mathrm{i}\,\omega\varepsilon_0\varepsilon\mathbf{E}, \tag{1}$$

for the electric and magnetic fields $\mathbf{E} = (E_x, E_y, E_z)$ and $\mathbf{H} = (H_x, H_y, H_z)$ respectively. ε_0 and μ_0 are the vacuum permittivity and permeability, $\varepsilon(x, y, z) = n^2(x, y, z)$ is the relative dielectric permittivity. The relative permeability μ is assumed to be one, as is appropriate for most materials at optical frequencies.

Solutions $(\mathbf{E}, \mathbf{H})$ of Equation (1) are stationary points of the functional [6]

$$\mathfrak{F}(\mathbf{E}, \mathbf{H}) = \int \left(\mathbf{E} \cdot (\nabla \times \mathbf{H}) + \mathbf{H} \cdot (\nabla \times \mathbf{E}) - \mathrm{i}\,\omega\varepsilon_0\varepsilon\mathbf{E}^2 + \mathrm{i}\,\omega\mu_0\mu\mathbf{H}^2 \right) \mathrm{d}x\,\mathrm{d}y\,\mathrm{d}z. \tag{2}$$

In the following, we will work with this variational formulation only.

3. VARIATIONAL EFFECTIVE INDEX METHOD

Let us consider only one TE slab mode propagating in the direction z with propagation constant $\beta_{\rm r}$ from a reference slice with permittivity distribution $\varepsilon_{\rm r}(x)$:

$$\begin{pmatrix} E_x, E_y, E_z \\ H_x, H_y, H_z \end{pmatrix}_{\rm slab}(x, z) = \begin{pmatrix} 0, & X^{E_y}(x), & 0 \\ X^{H_x}(x), & 0, & X^{H_z}(x) \end{pmatrix} \cdot e^{-{\rm i}\,\beta_{\rm r} z}, \tag{3}$$

The principal electric component X^{E_y} satisfies the equation

$$\left(X^{E_y}(x)\right)'' + k^2 \varepsilon_{\rm r}(x) X^{E_y}(x) = \beta_{\rm r}^2 X^{E_y}(x) \tag{4}$$

with vacuum wavenumber $k = 2\pi/\lambda$. The remaining two nonzero components of the mode profile can be derived directly from X^{E_y}.

We assume that this vertical shape constitutes an adequate approximation for the (polarized) optical field in the 3D structure

$$\begin{pmatrix} E_x, E_y, E_z \\ H_x, H_y, H_z \end{pmatrix}_{\rm complete}(x, y, z) = \begin{pmatrix} 0, & X^{E_y}(x)P^{E_y}(y, z), & X^{E_y}(x)P^{E_z}(y, z) \\ X^{H_x}(x)P^{H_x}(y, z), & X^{H_z}(x)P^{H_y}(y, z), & X^{H_z}(x)P^{H_z}(y, z) \end{pmatrix}, \tag{5}$$

with some unknown functions P. Note that the y- and z-components of the electromagnetic field are approximated by the same functions X.

The governing equations for the functions P can be found by restricting the functional (2) to the template (5), i.e., by requiring, after insertion of (5) into (2), the variations of $\mathfrak{F}$ with respect to all P to vanish. Using the relations between the slab mode components, it turns out that P^{H_x} satisfies the following second order differential equation

$$\left(\partial_y \frac{1}{\varepsilon_{\rm eff}(y, z)}\partial_y + \partial_z \frac{1}{\varepsilon_{\rm eff}(y, z)}\partial_z + k^2\right) P^{H_x}(y, z) = 0 \tag{6}$$

with

$$\varepsilon_{\rm eff}(y, z) = \frac{\beta_{\rm r}^2}{k^2} + \frac{\displaystyle\int \left(\varepsilon(x, y, z) - \varepsilon_{\rm r}(x)\right)\left(X^{E_y}(x)\right)^2 \, dx}{\displaystyle\int \left(X^{E_y}(x)\right)^2 \, dx}. \tag{7}$$

This looks exactly like a 2D TM Helmholtz equation with (effective) permittivity $\varepsilon_{\rm eff}$, and similar to what is used in the standard Effective Index Method. In the reference slice, where $\varepsilon(x, y, z) = \varepsilon_{\rm r}(x)$, the effective permittivity is equal to the squared effective mode index $\beta_{\rm r}^2/k^2$. Elsewhere, however, this squared effective index is modified by the difference between the local permittivity and that of the reference slice, weighted by the local intensity of the major component of the reference mode profile. Hence, contrary to the EIM, even in slices where no guided mode exists the effective indices are still rigorously defined.

Note that the original problem (2) deals with six unknown field components, each depending on three spatial coordinates. The present approximation reduced it to a single function of two spatial coordinates only.
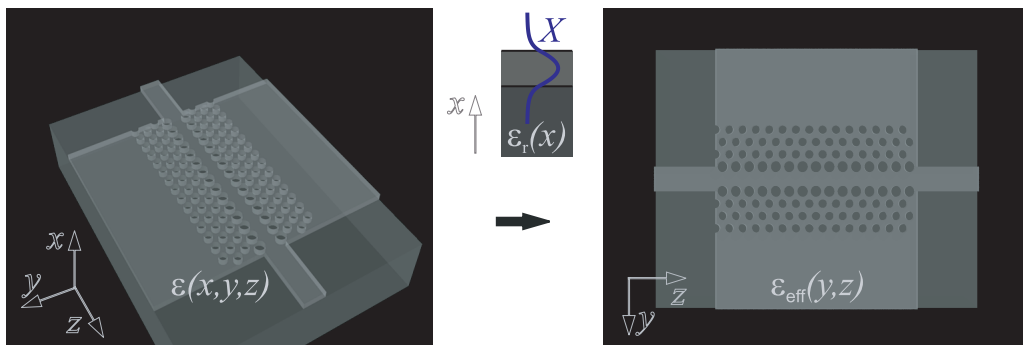

Figure 1: By using a TE slab mode of a reference slice with permittivity $\varepsilon_{\rm r}(x)$ as an approximation for the x-dependence of the field, the simulation of wave propagation in the structure is reduced from 3D to 2D.

All other field components are related to P^{H_x} in the following manner:

$$\begin{pmatrix} P^{E_x}, P^{E_y}, P^{E_z} \\ P^{H_x}, P^{H_y}, P^{H_z} \end{pmatrix}(y,z) = \frac{\mathrm{i}\,\beta_\mathrm{r}}{k^2 \varepsilon_\mathrm{eff}} \begin{pmatrix} 0, & \partial_z P^{H_x}, & -\partial_y P^{H_x} \\ (-\mathrm{i}\,k^2 \varepsilon_\mathrm{eff}/\beta_\mathrm{r}) P^{H_x}, & \partial_y P^{H_x}, & \partial_z P^{H_x} \end{pmatrix}. \tag{8}$$

Equation (8) permits a quite intuitive interpretation. Inside each homogeneous region a partial solution of (6) is

$$P^{H_x}(y,z) = c\, \mathrm{e}^{-\mathrm{i}\,(k_y y + k_z z)}, \quad \text{with} \quad k_y^2 + k_z^2 = k^2 \varepsilon_\mathrm{eff}. \tag{9}$$

If we define $\rho^2 = k^2 \varepsilon_\mathrm{eff}$, and an angle θ such that $\cos\theta = k_z/\rho$ and substitute it in (8), we obtain

$$\begin{pmatrix} P^{E_x}, P^{E_y}, P^{E_z} \\ P^{H_x}, P^{H_y}, P^{H_z} \end{pmatrix}(y,z) = c\frac{\beta_\mathrm{r}}{\rho}\, \mathrm{e}^{-\mathrm{i}\,\rho(-\sin\theta y + \cos\theta z)} \begin{pmatrix} 0, & \cos\theta, & \sin\theta \\ \frac{\rho}{\beta_\mathrm{r}}, & -\sin\theta, & \cos\theta \end{pmatrix}. \tag{10}$$

In the reference slice we have $\rho = \beta_\mathrm{r}$, and hence the functions P act as a rotation of the slab mode around the x-axis. In all other regions, in addition to the rotation of the y- and z-components, the x-component is scaled by ρ/β_r.

Moreover, as (10) is only a partial solution and the fundamental solution of (6) is a superposition of partial solutions, the functions P (8) act as a superposition of the slab mode X rotated around the x-axis by different angles θ.

So far, the formulation has not been restricted to a computational domain, and Equation (6) holds in entire $\mathbb{R}^2$. In practice, however, solving (6) requires a finite computational window, with boundaries such that influx can be prescribed and radiation can freely flow out. We use a modified version of the Transparent Influx Boundary Conditions from [3, 5] which fulfill these requirements. In this scheme, a finite element calculation of the field in the interior of the domain is connected to a semi-analytical solution of the exterior.

4. NUMERICAL RESULTS

In this section, we compare the results of EIM, VEIM and 3D FDTD [2] -simulations of the photonic crystal waveguide of Figure 1, for the following specification: The structure is composed of a 225 nm thick Si ($n_\mathrm{Si} = \sqrt{12.1}$) layer on top of a SiO$_2$ ($n_\mathrm{SiO_2} = 1.445$) substrate with air ($n_\mathrm{air} = 1.0$) around. The waveguide and holes are defined by etching fully through the Si layer. The triangular lattice photonic crystal with lattice constant $a = 440$ nm consists of circular holes with radius 135 nm; the input and output waveguides are $\sqrt{3}a \approx 762$ nm wide. A defect waveguide is created by removing a row of holes and enlarging the first row of holes on either side to a radius of 170 nm. In total, there are four rows of holes on either side of the defect waveguide.

This geometry is particularly interesting because no guided mode exists in the vertical slices, where holes are located. So to apply 'standard' EIM one has to guess the effective refractive index of
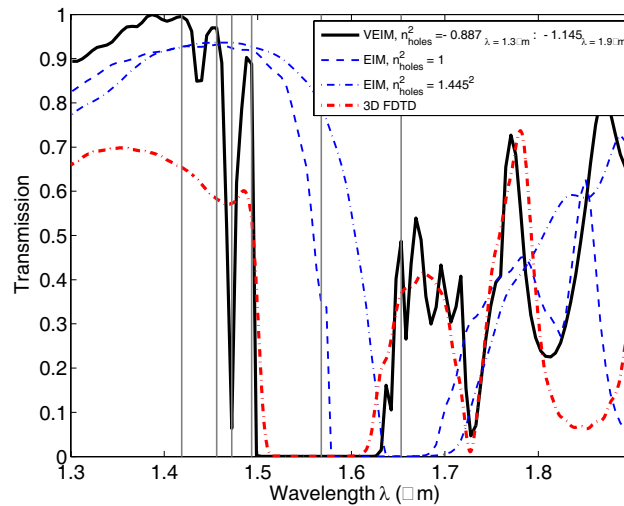

Figure 2: Transmission spectrum of the photonic crystal waveguide shown in Figure 1.
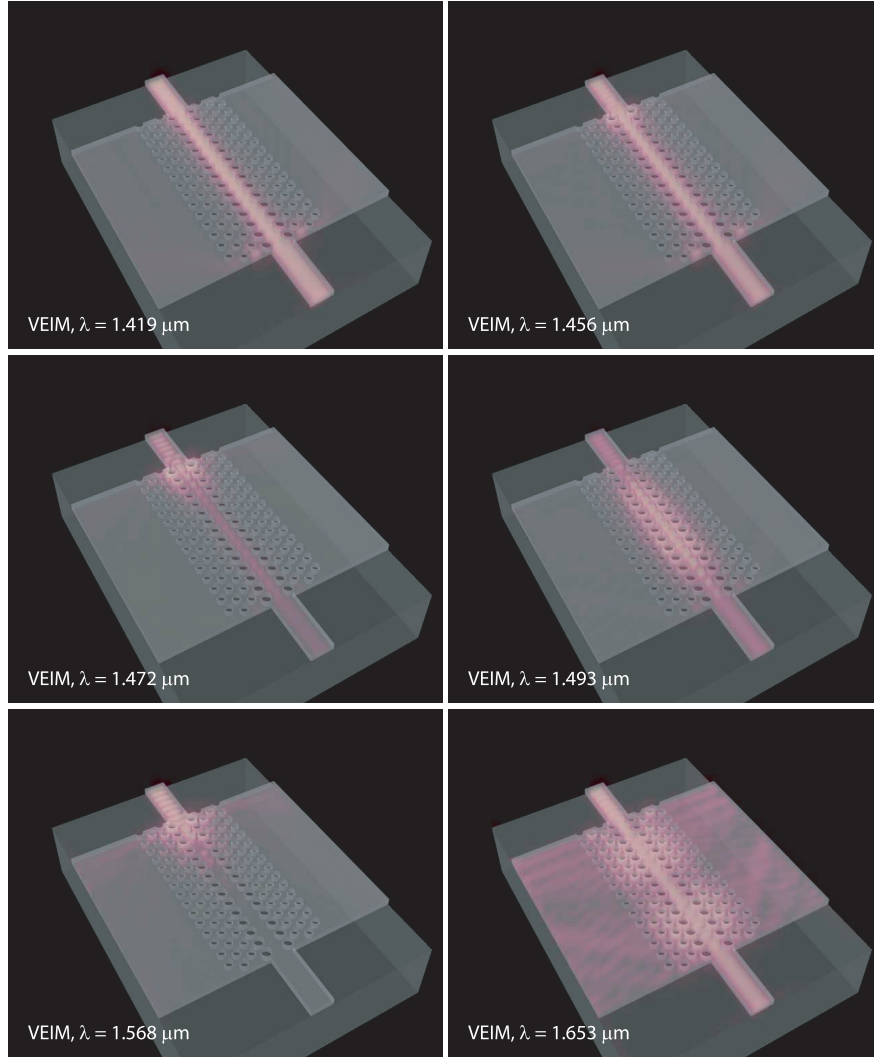
Figure 3: 3D light propagation through the photonic crystal slab waveguide of the Figure 1 at several vacuum wavelengths; absolute value of the major magnetic component of the optical field.

those regions: should it be the refractive index of the Si substrate or air, or something in between? VEIM uniquely defines these numbers.

As shown in Figure 2, the VEIM predictions of the location of the stopband and the general spectral features are reasonably close to the 3D FDTD reference results, while the 'conventional' EIM data, using either the cladding (1.0) or substrate refractive indices (1.445) as effective values for the hole regions, are much further off. Via the template (5), the VEIM allows to assemble an approximation to the vectorial electromagnetic field in 3D. Figure 3 shows a series of corresponding field profiles. Note that the effective permittivity (7) can very well turn out to be negative, as it happens to be in the present example. Inside the hole regions the effective permittivity varies between $-0.887_{@\lambda=1.3\,\mu m}$ and $-1.145_{@\lambda=1.9\,\mu m}$. So in all air regions in Figure 3 the field H_x decays exponentially.

5. CONCLUDING REMARKS

The present technique allows in a straightforward and simple way reduce the dimensionality of the scattering problems from 3D to 2D for TE-like polarized light. A similar procedure has also been developed for TM polarization. Currently, work is in progress to extend the method to deal with the third dimension even more accurately, by means of superpositions of contributions of the form (5) related to multiple slab modes.

ACKNOWLEDGMENT

REFERENCES

1. Dems, M. and W. Nakwaski, "The modelling of high-contrast photonic crystal slabs using the novel extension of the effective index method," *Optica Applicata*, Vol. 36, No. 1, 51–56, 2006.
2. MEEP, "Free finite-difference time-domain simulation software package developed at MIT," http://www.ab-initio.mit.edu/meep.
3. Nicolau, J. B. and E. van Groesen, "Hybrid analytic-numeric method for light through a bounded planar dielectric domain," *Journal of Nonlinear Optical Physics and Materials*, Vol. 14, No. 2, 161–176, 2005.
4. Qiu, M., "Effective index method for heterostructure-slab-waveguide-based two-dimnsional photonic crystals," *Applied Physics Letters*, Vol. 81, No. 7, 1163–1165, 2002.
5. Stoffer, R., A. Sopaheluwakan, M. Hammer, and E. van Groesen, "Helmholtz solver with transparent influx boundary conditions and nonuniform exterior," *Proc. of XVI International Workshop on Optical Waveguide Theory and Numerical Modelling*, Copenhagen, Denmark, 2007. book of abstracts 3.
6. Vassallo, C., *Optical Waveguide Concepts*, Elsevier, Amsterdam, 1991.
7. Yang, L., J. Motohisa, and T. Fukui, "Suggested procedure for the use of the effective-index method for high-index-contrast photonic crystal slabs," *Optical Engineering*, Vol. 44, No. 7, 078002-1–078002-7, 2005.